

Unsteady Aerodynamic Simulations of Floating Offshore Wind Turbines with Overset Grid Technology

Ping Cheng¹, Decheng Wan^{1*} and Changhong Hu²

1 State Key Laboratory of Ocean Engineering, School of Naval Architecture, Ocean and Civil Engineering, Shanghai Jiao Tong University, Collaborative Innovation Center for Advanced Ship and Deep-Sea Exploration, Shanghai, China

2 Research Institute for Applied Mechanics, Kyushu University, Fukuoka, Japan

* Corresponding author

ABSTRACT

The aerodynamic performance of the floating offshore wind turbine has an extra level of complexity than that of bottom-fixed wind turbines because of the motions of the supporting platform. In this paper, the unsteady aerodynamic performance of the NREL-5MW Baseline wind turbine with periodical surge and pitch motions of its supporting platform are investigated. The three-dimensional Reynolds Averaged Navier-Stokes equations are solved for the aerodynamic numerical simulation. The naoe-FOAM-os-SJTU solver, which is based on OpenFOAM and overset grid technology and developed for ship and ocean engineering problems, is employed. From the simulation, the time series of the unsteady torque and thrust are obtained, together with the detailed information of the wake flow field, and the pressure coefficient distribution in different cross-section are also available to clarify the detailed flow field information. The simulation results are compared both with those obtained from aerodynamic simulation of wind turbine without effects of platform motions, and with other approaches in previous studies. The simulation results show that the pitch motion has more significant effects on the aerodynamic forces and moments of the rotor than the surge motion does. And the motion of the platform especially the pitch motion may bring very bad influence on the turbine forces and wake flow, even on the power generation in case of very severe pitch motion.

KEY WORDS: unsteady aerodynamic simulation; floating offshore wind turbine (FOWT); overset grid technology; naoe-FOAM-os-SJTU solver.

INTRODUCTION

As renewable and sustainable, wind energy represents a potential to solve the energy and environment crisis, especially for the coastal countries which have enormous ocean wind energy resource. With special and strong advantages over onshore or fixed-bottom offshore wind turbines, floating offshore wind turbines (FOWT) become more and more competitive. But environment loads on FOWTs have an extra level of complexity, among which the aerodynamic loads are of great significance.

Since the onshore wind turbines were widely used much earlier, there exist many kinds of methods for the aerodynamic simulation of a wind

turbine. The three main method for the aerodynamic performance simulation of the wind turbines, which are the Blade Element Momentum theory (BEM), the Generalized Dynamic Wake model (GDW) and the Computational Fluid Dynamics (CFD), are well developed for the steady aerodynamic simulation of the fixed-bottom wind turbine, among which BEM and CFD are also developed for unsteady simulations.

But the aerodynamic performance of the floating offshore wind turbines differs a lot from that of bottom-fixed wind turbines. Compared with onshore wind turbine or fixed offshore wind turbine, the floating offshore wind turbines (FOWTs) work in much more complex environment. The environment forces on the FOWTs become more complicated than those on the bottom-fixed wind turbine. Coupled with motion of the floating platform, the aerodynamic forces on the wind turbine become more unsteady, and the unsteady aerodynamic simulation of the FOWTs are even more important.

Tran, et al. (2014) illustrated the unsteady aerodynamics of a floating offshore wind turbine with prescribed sinusoidal pitch motion of the platform using overset grid technique in Star-CCM+, which indicates 30% increase of thrust and 100% increase of power with a 4° pitch motion with 0.1Hz frequency of the platform. Li, et al. (2015) conducted the unsteady simulation of a 5-MW wind turbine with both predicted sinusoidal surge motion and pitch motion of the platform respectively. The unsteady actuator line model (UALM) is used, and predicted that the pitch motion of the platform has more significant influence on the aerodynamic characters of the rotor than the surge motion.

In this paper, the unsteady aerodynamic performance of the NREL-5MW Baseline wind turbine with periodical surge and pitch motions of its supporting platform are investigated. The three-dimensional Reynolds Averaged Navier-Stokes equations are solved for the aerodynamic numerical simulation. The naoe-FOAM-os-SJTU solver (Shen and Wan, 2015), which is based on OpenFOAM and overset grid technology and developed for ship and ocean engineering problems, is employed. From the simulation, the time series of the unsteady torque and thrust are obtained, together with the detailed information of the wake flow field, and the pressure coefficient distribution in different cross-section are also obtained to clarify the detailed flow field information.

MATHEMATICAL MODEL AND NUMERICS

Overset Grid Technique

The solver used in this paper is our in-house code naoe-FOAM-os-SJTU (Shen and Wan, 2015), which is compiled by implementing the dynamic overset grid technique into the OpenFOAM-based solver naoe-FOAM-SJTU (Shen et al., 2012; Shen and Wan, 2013).

Using overset grid technique, the separate overlapping grids for each part with independent motion are allowed, which makes it a good method for simulation of large amplitude motion problems. And the connection among grids of each part is built by interpolation at appropriate cells or points using DCI (domain connectivity information) which is produced by SUGGAR++. (Noack, R.W. 2005b. Carrica, et al. 2010b). There are four main steps when using DCI in the overset grid technique: The first step is to mark the hole cells which are located outside the simulation domain or of no interest, and exclude them from computation. As shown in Fig.1, in each overset grid, there exist series of cells around hole cells named fringe cells, and for each fringe cell there are several donor cells which provide information from the donor grids, so the second step is to seek for the donor grids of each fringe cell and provide information from the donor grids. The third step is to obtain the value of a variable ϕ of the fringe cell by interpolation using Eq.1 from the donor cells find in the second step.

$$\phi_i = \sum_{i=1}^n \omega_i \cdot \phi_i \quad (1)$$

Where ϕ_i is the value of a variable ϕ of the fringe cell, ϕ_i is the value for the i^{th} donor cell, ω_i is the weight coefficient, which is dimensionless and follows the condition shown in Eq.2:

$$\sum_{i=1}^n \omega_i = 1 \quad (2)$$

And the last step is to optimize the overlapping area and improve the accuracy of interpolation.

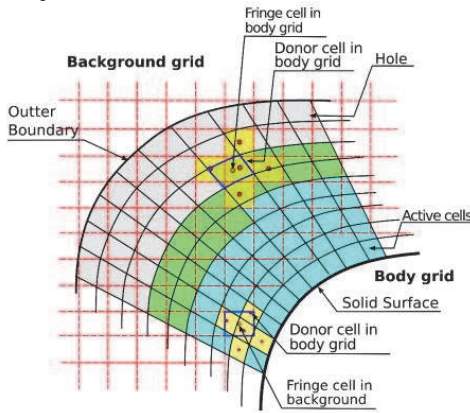


Fig. 1 Diagram of overset grid

Governing Equations

The governing equation solved in this paper is the incompressible Reynolds-Average Navier-Stokes (RANS) equations which can be written as:

$$\frac{\partial U_i}{\partial x_i} = 0 \quad (3)$$

$$\frac{\partial U_i}{\partial t} + \frac{\partial}{\partial x_j} (U_i U_j) = -\frac{1}{\rho} \frac{\partial P}{\partial x_i} + \frac{\partial}{\partial x_j} \left(\nu \frac{\partial U_i}{\partial x_j} - u_i u_j \right) \quad (4)$$

Where U is the velocity of flow; ρ is the density of the fluid; p is the pressure; ν is the kinematic viscosity.

To solve the governing Eq.3-4, the $k-\omega$ SST turbulence model (Menter, 1994) is employed, in which the turbulent kinetic energy k and the turbulent dissipation rate ω can be described as:

$$\frac{\partial}{\partial t} (\rho k) + \frac{\partial}{\partial x_i} (\rho k u_i) = \frac{\partial}{\partial x_j} \left(\Gamma_k \frac{\partial k}{\partial x_j} \right) + G_k - Y_k + S_k \quad (5)$$

$$\frac{\partial}{\partial t} (\rho \omega) + \frac{\partial}{\partial x_i} (\rho \omega u_i) = \frac{\partial}{\partial x_j} \left(\Gamma_\omega \frac{\partial \omega}{\partial x_j} \right) + G_\omega - Y_\omega + D_\omega + S_\omega \quad (6)$$

Where, Γ_k and Γ_ω are the effective diffusion coefficients for the turbulent kinetic energy k and the turbulent dissipation rate ω respectively, G_k and G_ω are turbulence generation terms, Y_k and Y_ω are turbulent dissipation terms, D_ω is the cross-diffusion term for ω , S_k and S_ω are the source term.

SIMULATION SETUP

Geometry model and grids

Phase II of OC4 project involving modeling of NREL 5MW Baseline Wind Turbine (Jonkman et al. 2009) and the semi-submersible floating offshore wind system (Robertson et al, 2012) is chosen in this paper, which is shown below in Fig.2.

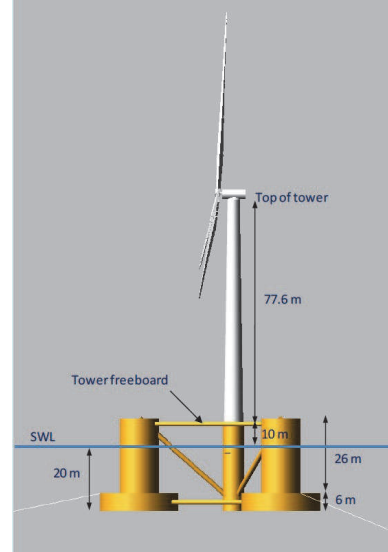


Fig. 2 The Phase II of OC4 floating wind turbine

As shown in Fig.2, The Phase II of OC4 floating wind turbine consists of two main parts: the turbine with tower in air and the semi-submersible platform with mooring lines in water. In this paper, the hydrodynamic performance of the floating platform is not computed directly, but its impact on the wind turbine is considered by simplified the motion of the platform as a predicted sinusoidal motion in surge or pitch directions.

Table.1 gives some properties of the NREL 5MW Baseline Wind Turbine used in this paper, and Table.2 and Table.3 show the structural properties of the blades and the tower respectively.

Table 1. Summary of the NREL 5MW Baseline Wind Turbine properties

Rating	5MW
Wind Regime	IEC 61400-3 (Offshore) Class 1B / Class 6 winds
Rotor Orientation	Upwind
Control	Variable Speed, Collective Pitch
Rotor Diameter / Hub Diameter	126m / 3m
Hub Height	90m
Maximum Rotor / Generator Speed	12.1rpm / 1,173.7rpm
Maximum Tip Speed	80m/s
Overhang / Shaft Tilt / Precone	5m / 5° / 2.5°

Table 2. Summary of the Blade Structural Properties

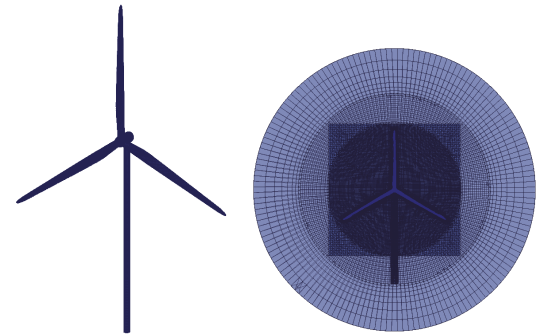
Length (w.r.t. Root Along Preconed Axis)	61.5m
Mass Scaling Factor	4.536%
Overall (Integrated) Mass	17,740 kg
Second Mass Moment of Inertia (w.r.t. Root)	11,776,047 kg-m ²
First Mass Moment of Inertia (w.r.t. Root)	363,231 kg-m
c.g. Location (w.r.t. Root Along Preconed Axis)	20.475m
Structural Damping Ratio (All Modes)	0.477465%

Table 3 Tower Properties

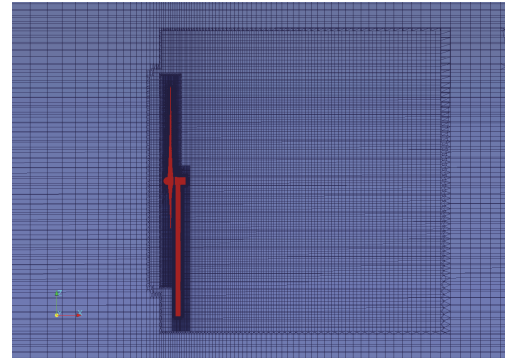
Height above Ground	61.5m
Overall (Integrated) Mass	347,467 kg
CM Location (w.r.t. Ground along Tower Centerline)	20.475m
Structural Damping Ratio (All Modes)	1%

With these structural properties and the detailed data of blade (Lindenburg, C.,2002), the structural model is built with CATIA, which is shown in Fig.3(a). According to the structural properties listed in Table.1-3, the simulation domain is generated as a cylinder, which is shown in Fig.3(b-c). The radius of the cylinder domain is about 2R, where R is the radius of the rotor, and length is 240m, which is about 4R. The distance between the model and the inlet boundary is 60m, and the distance between the model and the outlet boundary is 240m. To improve the simulation accuracy, refinement of the mesh around turbine and tower is necessary, and proper mesh refinement in the wake flow field is also very important to capture the flow information in the wake flow.

To use the overset grid technique, three overlapping meshes are generated, which are the background mesh of the simulation domain generated with ICM-CFD, and the overlapping grids for the rotor and tower generated with anappyHexMesh supplied with OpenFOAM respectively.



(a) structural model (b) side view of grid structure



(c) grid structure

Fig. 3 Geometry Model and Grid Structure

Simulation Cases

In this paper, the aerodynamic simulation of the wind turbine is conducted with the impact of predicted sinusoidal motion of the floating platform both in surge and pitch directions. There are four cases selected in this paper, which are listed in Table.4. The wind speed in these simulations are constant which equals to the rated wind speed $U=11.4\text{m/s}$.

Table 4 simulation cases

	Motion Direction	Motion	Velocity
Case1	Surge	$X_{\text{Surge}}=4\sin(0.246*t)$	$U_x=0.984\cos(0.246*t)$
Case2	Surge	$X_{\text{Surge}}=8\sin(0.246*t)$	$U_x=1.968\cos(0.246*t)$
Case3	Pitch	$\theta_{\text{Pitch}}=4\sin(0.314*t)$	$\omega_{\text{Pitch}}=1.256\cos(0.314*t)$
Case4	Pitch	$\theta_{\text{Pitch}}=8\sin(0.314*t)$	$\omega_{\text{Pitch}}=2.512\cos(0.314*t)$

Fig.4-5 shows the motion in one period in each case. In Fig.4-5, the vertical axis shows the motion of the platform, and the horizontal axis named t/T is the dimensionless time value, where T represents the rotating period of the wind rotor, which can be obtained from the rated rotor speed shown in Table.1. In case1 and case2, the period of the platform surge motion is about 5.15 times of the rotating period of rotor, while in case3 and case4, the period of the pitch motion is about 4 times of the rotating period of rotor.

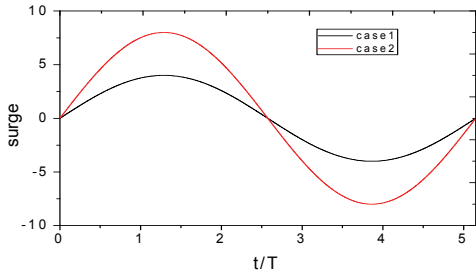


Fig.4 platform motion during one period in case1 and case2

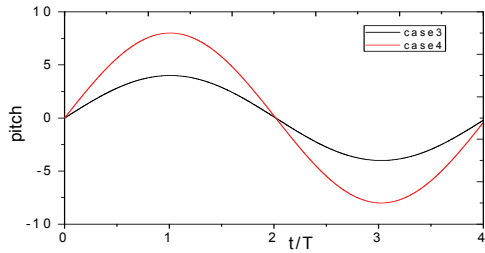


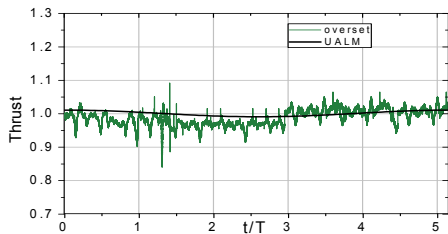
Fig.5 platform motion during one period in case3 and case4

RESULTS AND DISCUSSION

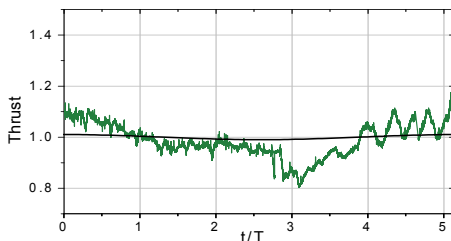
Rotor Thrust and Torque

From the simulation, the time history of unsteady thrust and torque of the wind turbine are obtained. The time history of thrust and torque are shown in Fig6-9. To analyze the effects on the rotor aerodynamic performance of different cases, the simulation results during the same period of surge or pith motion are picked out.

The non-dimensional treatment is done on the thrust and torque results by dividing the thrust or torque by the mean value. And the time value is also non-dimensional treated by dividing time with the rotating speed of rotor. As mentioned above, the period of the platform surge motion is about 5.15 times of the rotating period of rotor, while the period of the pitch motion is about 4 times of the rotating period of rotor.

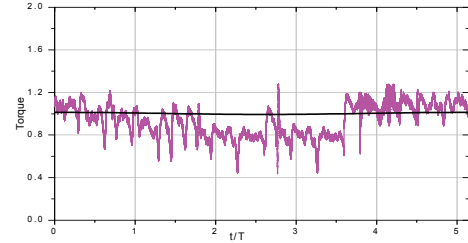


(a) Case1, Surge = $4\sin(0.246*t)$

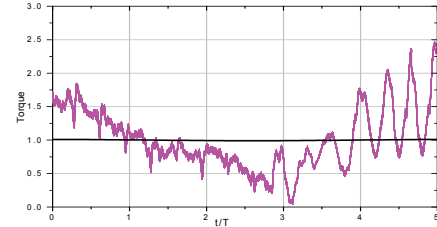


(b) Case2, Surge = $8\sin(0.246*t)$

Fig.6 Time History of Thrust with Surge motion of Platform

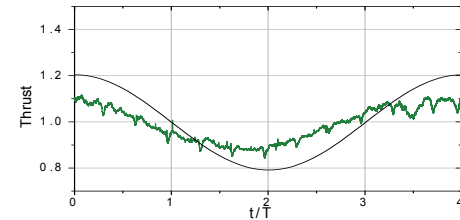


(a) Case1, Surge = $4\sin(0.246*t)$

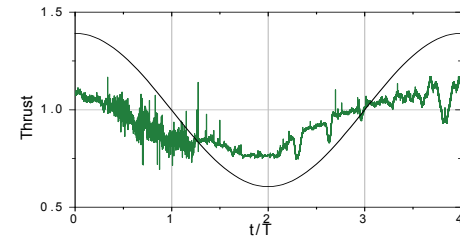


(b) Case2, Surge = $8\sin(0.246*t)$

Fig.7 Time History of Torque with Surge motion of Platform

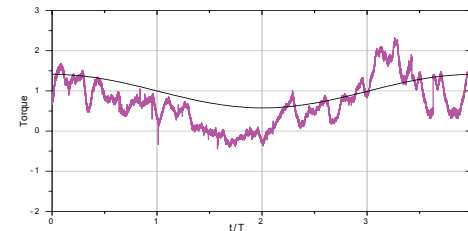


(a) Case3, Pitch = $4\sin(0.314*t)$

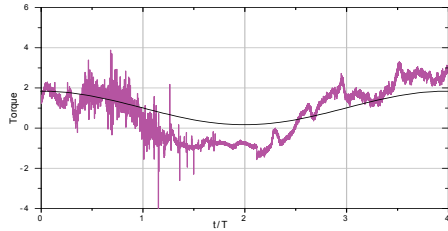


(b) Case4, Pitch = $8\sin(0.314*t)$

Fig.8 Time History of Thrust with Pitch motion of Platform



(a) Case3, Pitch = $4\sin(0.314*t)$



(b) Case4, Pitch = $8\sin(0.314*t)$

Fig.9 Time History of Torque with Pitch motion of Platform

In Fig6-9, some high frequency fluctuations are observed, which are believed to be caused by numerical simulation. The noisy phenomena even become more serious in case4. With prescribed surge or pitch motion of the platform, the turbine rotor moves periodically, which cause the change of the relative wind speed at every time step, so the numerical noisy appears. And when the turbine rotor moves forward to the wake, it interacts with its own wake flow, and the noisy phenomena get more serious.

In Fig6-9, the blue line and magenta line show the results obtained from our present work respectively. Fig.6 and Fig.8 show the time history of the thrust with predicted surge and pitch respectively. Both with surge motion and pitch motion, the effects of the platform motion improve obviously when the amplitude of the motion velocity increase. There is an interesting phenomenon that in most cases, three valleys can be observed during each one rotating period of rotor, which is believed to be caused by the tower effects, which was introduced in our earlier study (Ping, C. 2015).

Fig.7 and Fig.9 show the time history of the torque with predicted surge and pitch respectively. Similar conclusion can be obtained from the four figures of torque. The effects of the platform motion improve obviously when the amplitude of the motion increase. And the three valleys during each one rotating period caused by the tower effects can also be observed. It is noteworthy that the negative value of torque appears with platform motion in pitch direction, which has very bad influence on the generation power of the turbine. So we believe that the pitch motion of the platform should be avoid in normal working conditions of the wind turbine.

In Fig6-9, the black lines represent the results obtained with UALM method by Pengfei, et al (2015). In Fig6-7, the variable range of the black line is no more than 1%, while the variable range of the blue line is up to 20% and the range of the magenta line is over 50%. With surge motion of platform, the relative velocity changes to $U_r = U + U_{surge}$. The relative velocity varies in a range of (10.4~12.4) in case1 and a range of (9.4~13.4) in case2. The pressure on the surface of blade changes when the relative velocity changes, which causes change of the thrust and torque. Besides, the impact of tower also contributes to the large range of aerodynamic forces. Larger variable ranges are observed in Fig8-9 both from the results of UALM and the present work. The range occurs on the same principle, but the velocity of rotor in case3-4 increase a lot, so the variable ranges of aerodynamic forces increase obviously.

Pressure Coefficient

The pressure on the surface of the blades at different wind turbines were obtained from the simulation. And the pressure coefficient can be calculated with the pressure by Eq. 7:

$$C_p = \frac{P_0 - P_\infty}{0.5\rho[U^2 + (\omega r)^2]} \quad (7)$$

Where, P_0 represents the pressure obtained from the simulation, P_∞ is the pressure at infinity which is set as 0, ρ is the air density, U is the wind speed, ω is the rotating frequency, r is the rotating radius.

The pressure coefficients in case2 are analyzed in this paper. Fig.10-12 show the pressure coefficient on three cross sections of three blades at time $t=0.25T$, when the azimuth position is 463.5deg and one blade is very close to the tower. The first graph in Fig10-12 show the pressure coefficient on the three cross sections with steady aerodynamic simulation in our earlier study (Zhao W, 2014), and the rest three graphs show the pressure coefficient on the three blades. It should be noted that the pressure coefficient on the three blades are the same in the steady simulation without considering the effect of tower, while in this paper, the unsteady aerodynamic simulation is conducted, so the pressure coefficient on the three blades are not same any more, and also varies with the promoting of time. So not only the pressure coefficient on different cross section of different blades, but also those in different time are compared, shown in Fig13-15.

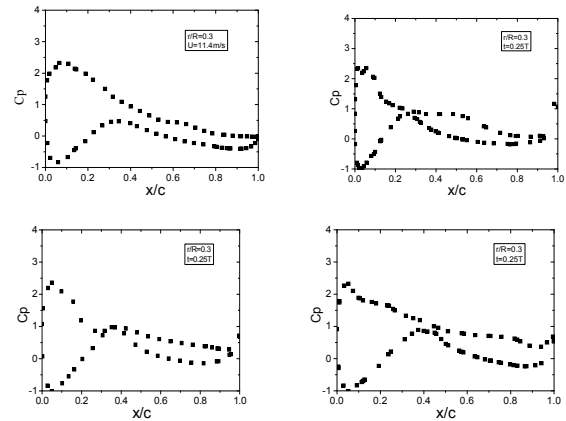


Fig.10 Pressure Coefficient at $r/R=0.3$, $t=0.25T$

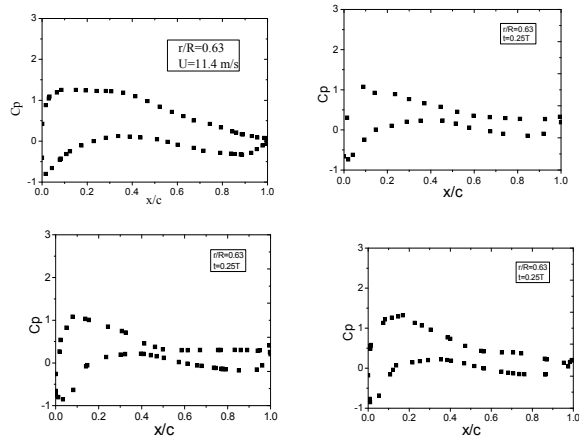


Fig.11 Pressure Coefficient at $r/R=0.63$, $t=0.25T$

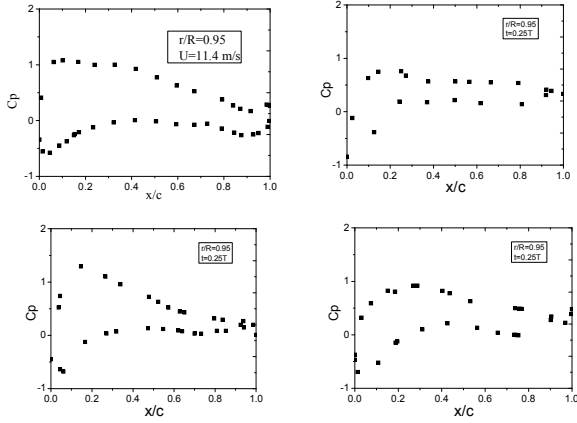


Fig.12 Pressure Coefficient at r/R=0.95, t=0.25T

Comparing the pressure coefficient curves on the three different cross sections of the blade, we can figure out that the pressure coefficient decreases as the r/R increases from 0 to 1. And the pressure coefficients on the same cross section of the three blades have similar values but still differ from each other, which is caused by the uneven distribution of the flow.

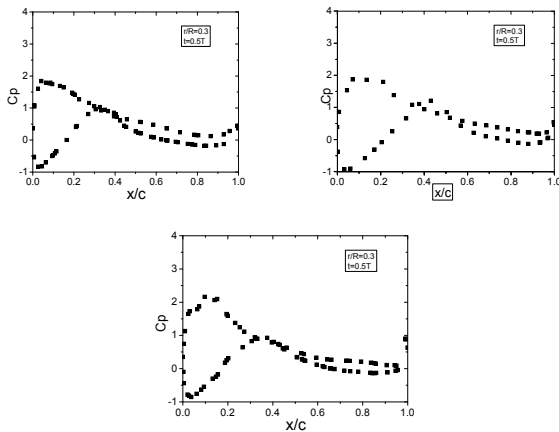


Fig.13 Pressure Coefficient at r/R=0.3, t=0.5T

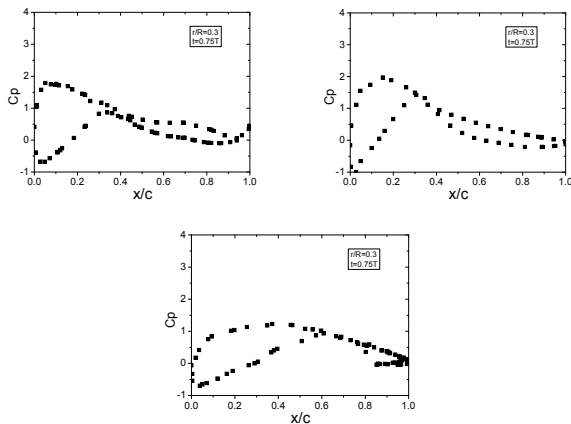


Fig.14 Pressure Coefficient at r/R=0.3, t=0.75T

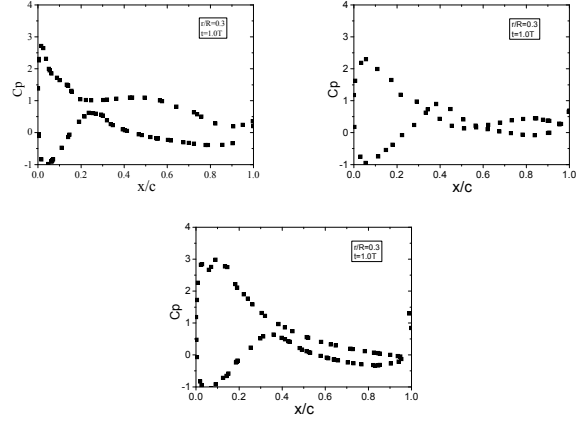


Fig.15 Pressure Coefficient at r/R=0.3, t=1.0T

Fig.10 and Fig.13-15 show the different pressure coefficient in four times during one surge period. Different from the steady simulation results, the pressure coefficient on the same cross section of the three blades change a lot with the time progressing, which also gives an proper explanation of the vary of the thrust and torque above.

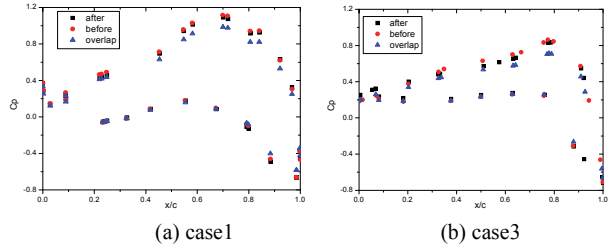


Fig.16 Pressure Coefficient at r/R=0.95 at Three Time Instants (before, after and during one blade overlapping the tower)

Fig.16 show pressure coefficient at r/R=0.95 at three time instants (before, after and during one blade overlapping the tower) in case1 and case3. From the figures, we can see that the pressure decreases when the blade overlaps the tower, which causes the decrease of thrust and torque at the same time.

Wake Vortex

The wake vortex structure is a very important index in the aerodynamic analysis of wind turbine, because the wake vortex near the blades has great influence on the aerodynamic properties of the blades. To get a proper wake vortex visualization result, the second invariant of the velocity gradient tensor, Q (Digraaskar D A, 2010), is used to capture the iso-surface of the vortex, which is:

$$Q = \frac{1}{2}(\Omega_{ij} \times \Omega_{ij} - S_{ij} \times S_{ij}) \quad (3)$$

In which the Ω_{ij} represents the strength of the vortex, and S_{ij} the shear strain rate.

The evolution of wake vortex at different time (0.25T, 0.5T, 0.75T, 1.0T) of a surge period or pitch period is illustrated in Fig.18-21. Fig.17 also gave the wake vortex obtained from both steady simulation without tower and unsteady simulation with tower.

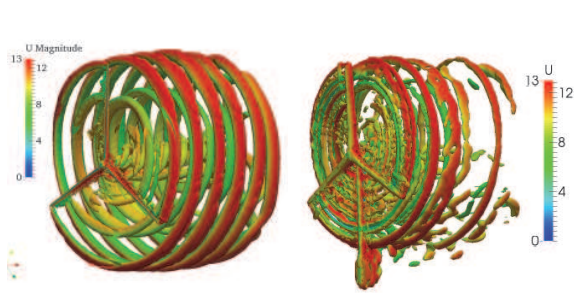
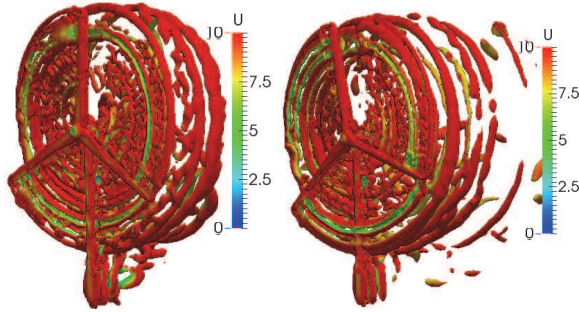
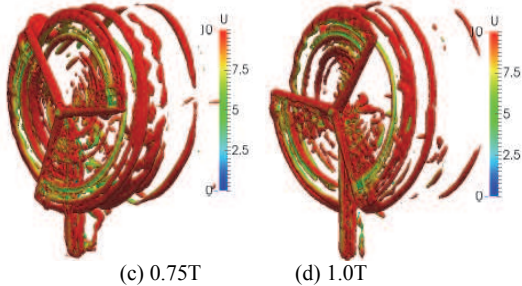


Fig.17 Wake Vortex of Fixed Turbine

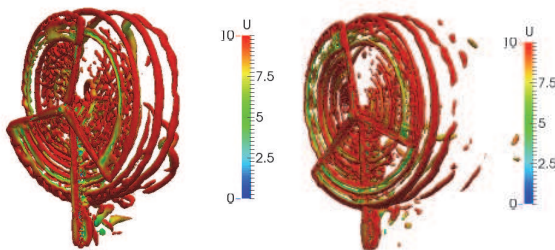


(a) 0.25T (b) 0.5T

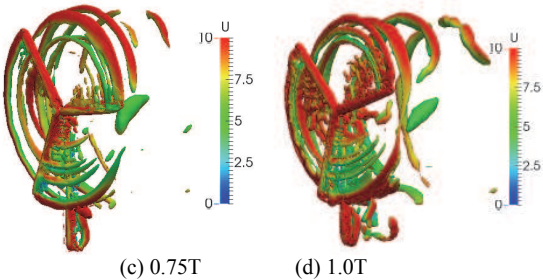


(c) 0.75T (d) 1.0T

Fig.18 Wake Vortex of Turbine with Surge motion of Platform (Surge = $4\sin(0.246*t)$)



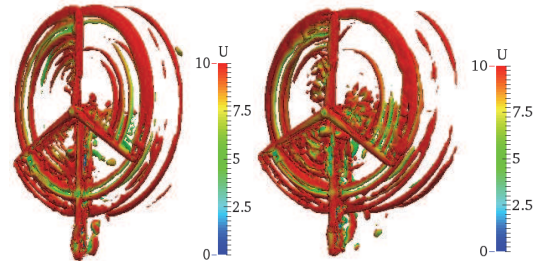
(a) 0.25T (b) 0.5T



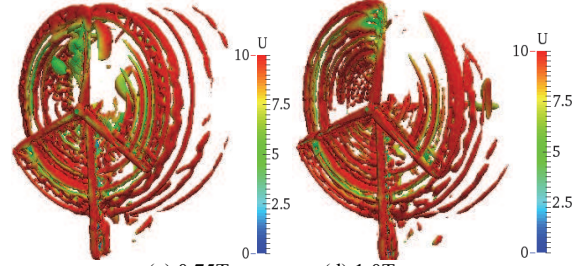
(c) 0.75T (d) 1.0T

Fig.19 Wake Vortex of Turbine with Surge motion of Platform (Surge = $4\sin(0.246*t)$)

$$= 8\sin(0.246*t)$$

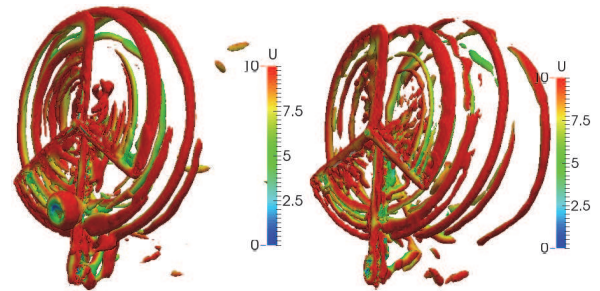


(a) 0.25T (b) 0.5T

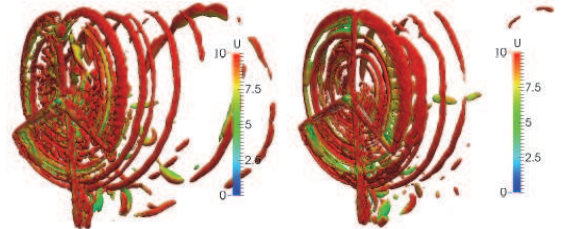


(c) 0.75T (d) 1.0T

Fig.20 Wake Vortex of Turbine with Pitch motion of Platform (Pitch = $4\sin(0.314*t)$)



(a) 0.25T (b) 0.5T



(c) 0.75T (d) 1.0T

Fig.21 Wake Vortex of Turbine with Pitch motion of Platform (Pitch = $8\sin(0.314*t)$)

Comparing Fig.18-21 with Fig.17, we can figure out that the motion of the platform makes the wake vortex more unsteady. When the turbine moves forward the wake flow, the density of vortex increases, while the turbine departs from the wake flow, the vortex structure becomes sparse. Similar to the conclusion obtained above, the pitch motion makes a higher unsteady character of the wake flow, than the surge motion does, which indicates that the pitch motion of the platform has a much greater influence on the wake flow of the turbine. And for both surge motion and pitch motion, the increase of the amplitude of the platform motion improves the unsteady character. In Fig.21 (a) we even find a vortex in front of the turbine, which is believed to be generated by the motion of the tower.

CONCLUSIONS

In this paper, the unsteady aerodynamic performance of the NREL-5MW Baseline wind turbine with periodical surge and pitch motions of its supporting platform are investigated. The three-dimensional Reynolds Averaged Navier-Stokes equations are solved for the aerodynamic numerical simulation. The naoe-FOAM-os-SJTU solver, which is based on OpenFOAM and overset grid technology and developed for ship and ocean engineering problems, is employed. From the simulation, the time series of the unsteady torque and thrust are obtained, together with the detailed information of the wake flow field, and the pressure coefficient distribution in different cross-section are also obtained to clarify the detailed flow field information. The simulation results are compared both with those obtained from aerodynamic simulation of wind turbine without effects of platform motions, and with other approaches in previous studies.

Very similar conclusions are obtained from the analysis of thrust and torque. The platform motion has significant effect on the aerodynamic forces and moments of the rotor. When the platform moves in surge or pitch direction, the relative velocity changes, so the aerodynamic forces and moments change at the same time. The effects of the platform motion improve obviously when the amplitude of the motion velocity increase. And the tower effect is observed from the thrust curves. It is noteworthy that with the platform motion in pitch direction, the negative value of torque appears, which has very bad influence on the generation power of the turbine. So we believe that the pitch motion of the platform should be avoid in normal working conditions of the wind turbine.

The detailed information of wake vortex and pressure coefficient distribution tells the same law with influence of the platform motion on the rotor aerodynamics. The motion of the platform especially the pitch motion may bring very bad influence on the turbine forces and wake flow, even on the power generation.

ACKNOWLEDGEMENTS

This work is supported by the National Natural Science Foundation of China (51379125, 51490675, 11432009, 51579145, 11272120), Chang Jiang Scholars Program (T2014099), Program for Professor of Special Appointment (Eastern Scholar) at Shanghai Institutions of Higher Learning (2013022), Innovative Special Project of Numerical Tank of Ministry of Industry and Information Technology of China (2016-23) and Foundation of State Key Laboratory of Ocean Engineering (GKZD010065), to which the authors are most grateful.

REFERENCES

Carrica P M, Huang J, Noack R, et al. Large-scale DES computations of the forward speed diffraction and pitch and heave problems for a surface combatant[J]. *Computers & Fluids*, 2010, 39(7): 1095-1111.

Cheng, P, Wan, DC (2015). Numerical Simulations of Complex Aerodynamic Flows around NREL Offshore 5-MW Baseline Wind Turbine[C]. Proceedings of the 9th International Workshop on Ship and Marine Hydrodynamics, Glasgow, UK.

Digraskar DA (2010). Simulations of flow over wind turbines[J]. Diffraction and pitch and heave problems for a surface combatant. *Comput. Fluids* 39 (7), 1095–1111.

Jonkman, J, Butterfield, S, Musial, W, Scott, G (2009). Definition of a 5-MW reference wind turbine for offshore system development.

Golden, CO: National Renewable Energy Laboratory.

Lindenburg C (2002). Aeroelastic modelling of the LMH64-5 blade[J]. Energy Research Center of the Netherlands, Technical Report No. DOWEC-02-KL-083/0, DOWEC 10083_001.

Li, P, Cheng, P, Wan, DC (2015). Numerical Simulation of Wake Flows of Floating Wind Turbines by Unsteady Actuator Line Model[C]. Proceedings of the 9th International Workshop on Ship and Marine Hydrodynamics, Glasgow, UK.

Menter FR(1994). Two-equation eddy-viscosity turbulence models for engineering applications[J]. *AIAA journal*, 32(8): 1598-1605.

Noack, RW (2005). SUGGAR: a general capability for moving body overset grid assembly. In: Proceedings of the 17th AIAA Computational Fluid Dynamics Conference, American Institute of Aeronautics and Astronautics, Toronto, Ontario, Canada.

Robertson, A, Jonkman, J, and Masciola, M (2012). "Definition of the Semisubmersible Floating System for Phase II of OC4." *Offshore Code Comparison Collaboration Continuation (OC4) for IEA Task*, 30.

Robertson, A, Jonkman, J and Musial W (2013). "Offshore Code Comparison Collaboration, Continuation: Phase II Results of a Floating Semisubmersible Wind System." *EWEA Offshore, Frankfurt, Germany*, no. NREL/CP-5000-60600.

Shen, Z, Cao, HJ and Wan, DC (2012). "Manual of CFD solver for ship and ocean engineering flows: naoe-FOAM-SJTU." Technical Report No. 2012SR118110, Shanghai Jiao Tong University.

Shen, Z, Wan, DC (2013). RANS computations of added resistance and motions of a ship in head waves. *Int. J. Offshore Polar Eng., ISOPE*, 23 (4), 263–271.

Shen, Z, Wan, DC, Carrica PM (2015). Dynamic overset grids in OpenFOAM with application to KCS self-propulsion and maneuvering[J]. *Ocean Engineering*, 108: 287-306.

Shen, Z and Wan, DC (2015). Manual of naoe-FOAM-os-SJTU Solver[R]. Technical Report No. 2015SR012974, Shanghai Jiao Tong University.

Tran, T, Kim D, Song, J (2014). Computational Fluid Dynamic Analysis of a Floating Offshore Wind Turbine Experiencing Platform Pitching Motion[J]. *Energies*, 7(8): 5011-5026.

Zhao, W, Cheng, P, Wan, DC (2014). Numerical Computation of Aerodynamic Performances of NREL Offshore 5-MW Baseline Wind Turbine[C]. The Proceedings of the Eleventh (2014) Pacific/Asia Offshore Mechanics Symposium (PACOMS-2014), Shanghai, China, October 12-16, 2014, ISOPE, pp. 13-18